

Flux-Gate Magnetometers Design Peculiarities

Valery Korepanov · Andriy Marusenkov

Received: 30 May 2011 / Accepted: 14 May 2012 / Published online: 1 June 2012
© Springer Science+Business Media B.V. 2012

Abstract The most widespread instrument used today for the measurement of quasi-stationary and slowly fluctuating vector magnetic fields is a flux-gate magnetometer (FGM). The most important parameter characterizing the magnetometer quality is its magnetic noise—its threshold sensitivity or its own noise level (NL). Based on the results of experimental research, we may state that the FGM NL mainly depends on the quality of the magnetic material used for FGM sensor core. The “solid liquid” model explaining the nature of magnetic noise is proposed and substantiated. It is demonstrated that special attention has to be paid to the annealing of the core. A new effect—termed gamma-magnetic normalization—is discovered and discussed. It is shown that the magnetometer NL depends not only on the core length and volume but also on the excitation mode of the core. Besides, the ways to improve other factors, such as power consumption and thermal drift which must be taken into account in order to create a FGM with the highest possible performance, are discussed. Some examples are given of the parameters of present advanced FGMs for geophysical uses.

Keywords Flux-gate magnetometer · Noise level · Power consumed · Excitation mode

1 Introduction

Measurements of the Earth’s magnetic field are probably the earliest metrological activity of mankind (Stern 2002), and progress in developing the methods used is impressive. While the first measurements of the Earth’s magnetic field were made with devices having a sensitivity threshold of about several tens of nanoTesla, the designers of magnetometers today have refined their resolution to the attoTesla level (Kominis et al. 2003). That is an improvement by about nine orders of magnitude! The technology first used to measure the geomagnetic field—via the mechanical force due to the interaction between a magnetized bar and the Earth’s magnetic field—is now complemented by numerous other methods of

V. Korepanov (✉) · A. Marusenkov
Lviv Centre of Institute for Space Research, 5-A Naukova Str., Lviv 79060, Ukraine
e-mail: vakor@isr.lviv.ua

magnetic field detection, as well as of magnetometer constructions. Between them, probably the most widely used magnetometers for the measurement of quasi-stationary and slowly fluctuating magnetic fields are flux-gate magnetometers.

Starting from the first publication related to FGMs (Aschenbrenner and Goubau 1936), a wealth of papers and books has been devoted to the different aspects of the special peculiarities of FGM operation. It is interesting to note that, despite the principle of operation and the main structure of a FGM remaining unchanged after its invention for more than 70 years, the number of publications in this field is not decreasing with time. Unfortunately, a great deal of the published papers contains similar information and re-discoveries in the field, which may partly be explained by the difficulties in the exchange of scientific information between Eastern and Western scientists, as well as by the still existing security aspects of military applications and by commercial-in-confidence considerations of FGMs. The recent growth of publications is probably triggered by the fact that, though some modern magnetometers using other physical principles may surpass FGMs in the most important parameter—noise—FGMs still remain the most convenient magnetometer for use today, especially in geophysics. The most significant progress was made by the creation of a fully digital FGM (e.g., Auster et al. 1995) and its miniaturization (Delevoeye et al. 2008). However, in order to create a FGM with the best possible performance, it is necessary to solve a set of scientific and technological problems aimed first of all at improving the FGM sensor. The aim of the present paper is to discuss the nature of the magnetic noise and to propose some procedures on how to decrease that. Some examples of the design of new FGMs are given in which the methods proposed to lower the NL and to reduce the power consumption are implemented.

2 Low-Noise FGM Design

2.1 Magnetic Noise

The most important parameter characterizing the magnetometer quality is magnetic noise level—this is due to fluctuations arising from the periodic magnetization of the flux-gate sensor (FGS) core. It determines the sensitivity threshold of a modern FGM (Musmann and Afanassiev 2010; Korepanov and Berkman 1999). The study of the NL characteristics has revealed that its spectral density $b(f)$ could be estimated by the following semi-empirical dependence (Berkman 1999):

$$b(f) = b_0[1 + (f_0/f)^\alpha], \quad (1)$$

where b_0 is the value of the spectral density at the frequency-independent (uniform) part of the spectrum; $f_0 \approx 1$ Hz is the changeover frequency; α is the coefficient of the spectral density slope at the frequencies below the changeover frequency f_0 , and f is the signal frequency.

The coefficient α is usually taken to be equal to 1 (Ripka 2001), although the values reported in the literature are spread in the range between 0.5 and 1.5 (Musmann and Afanassiev 2010). Detailed research on the NL frequency spectrum of the fluxgates and the magnetic modulators in the frequency range from 0.001 to 100 Hz has shown that the value of α has to lie between 0.75 and 0.8 (Berkman 1999). The authors' experience with FGM development and manufacturing confirms that the coefficient α lies in the range between 0.75 and 1.0 for properly designed instruments.

For ground geophysical surveys (e.g., geomagnetic observatories, magnetotelluric and magnetovariational soundings, etc.), FGMs are mainly used for measuring DC magnetic fields and slow fluctuations, because the strength of geomagnetic variations falls below most FGM NLs at the frequencies above about 0.1–1 Hz (Narod 2006). Thus, in the operational frequency band (from DC to 1 Hz) the FGM noise level depends on the frequency; it is important to know the sources of FGS noise components in this band. Let us therefore consider a simplified waveform model of fluxgate operation (Fig. 1).

The current I_{ex} passing through the primary coil creates a magnetizing force H_{ex} , which periodically saturates the magnetic core. The transition mode between the saturation states of the opposite polarity depends on the shape of the voltage across the primary coil (plots of B for the approximately rectangular shape are given in Fig. 1). The differential permeability of the magnetic material changes from its minimum value (approximately 1) during saturation states to the maximum value μ_{max} at small values of the magnetic induction B . For the measured field B_0 , the differential permeability of the core $\mu_{core}(t)$ varies similarly to this difference. Its maximum value is limited by the permeability of the shape μ_s due to the effect of the demagnetizing field (Musmann and Afanassiev 2010). Usually, $\mu_s < \mu_{max}$ and the waveform and spectrum of $\mu_{core}(t)$ may differ significantly from that of $\mu(t)$. In the presence of the measured field B_0 , the magnetic flux through the secondary coil changes proportionally to $\mu_{core}(t)$ generating the voltage $u_{sec}(t)$ across this coil. Ideally, in the case of perfect symmetry of the core and coils, the output voltage $u_{sec}(t)$ contains only even harmonics of the excitation frequency. In practice, however, there is asymmetry of the core halves and/or the primary and secondary coils so that odd harmonics appear in the voltage $u_{sec}(t)$ —this is the so-called “feed-through signal”. Besides the feed-through signal with a discrete spectrum, there is also the variation due to the magnetic noise. This noise signal is caused by the non-repeatability of the transitions

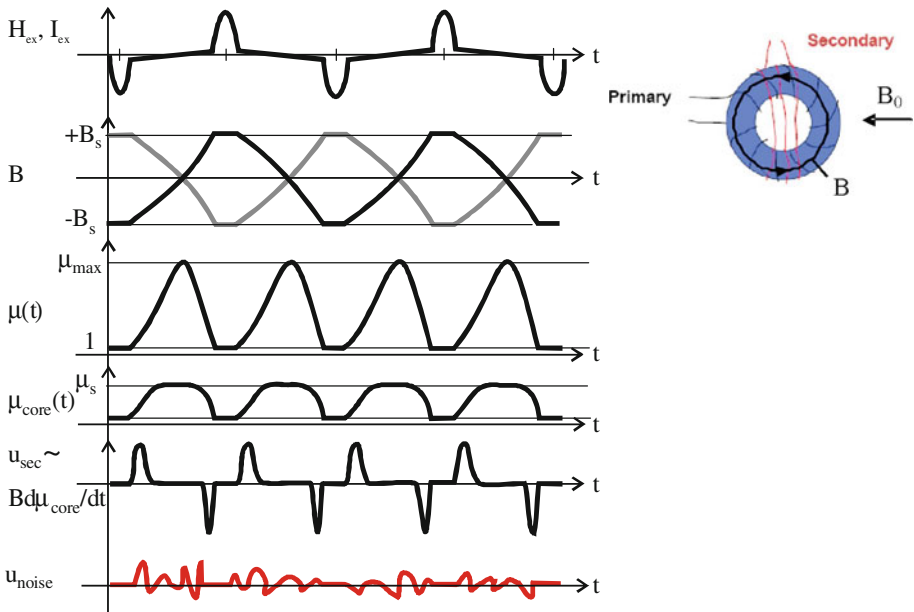


Fig. 1 Simplified model of fluxgate operation; the symbols are defined in the text

between the saturation states from cycle to cycle, which are often identified with fluctuations of the parameters of the Barkhausen jumps (Musmann and Afanassiev 2010). The approximate shape of the voltage $u_{\text{noise}}(t)$ across the secondary winding due to this noise signal is given in Fig. 1 (bottom plot). It is important to note that the intensity of the fluctuations is periodically dependent on time—the noise is non-stationary (Bittel 1969).

The variable intensity of the Barkhausen jumps was observed at different parts of the hysteresis loop (Bertotti et al. 1981; Bohn et al. 2007), as well as at the comparison of the same parts of the hysteresis loop taken during different cycles of excitation (Mykolaitis 1994). The authors' tests of the rod-core fluxgate with a Co-based amorphous magnetic core also revealed complex behavior of the hysteresis loop and its non-reproducibility from cycle to cycle (Fig. 2).

As shown in Fig. 2, the repeatability of magnetization reversal is better at the saturated states of the core, as one can expect based on the physical nature of magnetization. At deep saturation, the magnetic material is magnetized homogeneously and the saturation magnetization at a given temperature is basically defined by the material chemical composition (Liu et al. 2006). Let us note that to reach really deep saturation is not an easy task; for some materials, a huge magnetic field strength (hardly achievable in a conventional FGM) is necessary. For example, due to the surface defects of nanocrystalline (Flohrer et al. 2006) and amorphous (Amalou and Gijs 2001) tapes, magnetic domains with the opposite magnetization were observed for fields up to 20 kA/m. Thus, the well-known fact of the noise level decreasing with increasing excitation pulse amplitude (Musmann and Afanassiev 2010) may probably be explained by the improving repeatability of magnetization reversals at the greater saturation states.

2.1.1 Magnetic Materials Selection

The analysis and prediction of the magnetization processes is an extremely difficult task, because many factors have to be taken into account. The magnetization reversals between

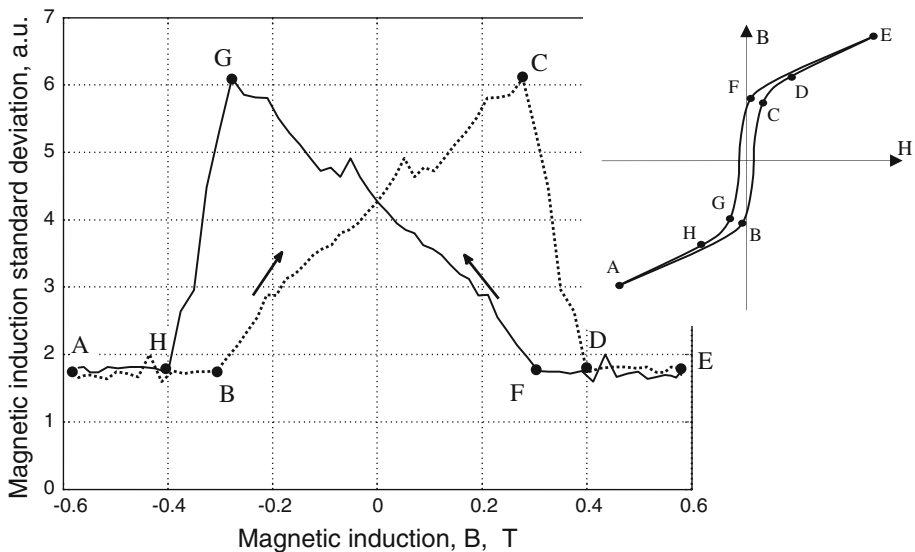


Fig. 2 Non-reproducibility of the hysteresis loop from cycle to cycle (*a.u.* arbitrary units)

the saturation stages are controlled by various mechanisms (phenomena): these include domain walls moving, coherent and incoherent rotations, annihilation and nucleation of domains as well as combinations of these processes (Liu et al. 2006). When the external field is zero, the distribution of the spontaneous magnetization directions is governed by the minimum of the free energy of exchange, magnetocrystalline, magnetoelastic, and magnetostatic interactions. Even with a homogenous external field, the distribution of the internal field could be inhomogeneous due to the demagnetizing effect. In the case of an AC magnetizing field, the physical picture becomes even more complicated due to the generation of micro and macro eddy currents, which create counter fields. Moreover, in a macroscopic magnetic system there are a number of structural imperfections such as grains in polycrystals, dislocations, chemical composition fluctuations, surface roughness. As a result, the energy landscape exhibits an extremely complicated structure. The magnetization \mathbf{M} is coupled to the external field \mathbf{H}_a by the energy $-\mu_0\mathbf{M}\mathbf{H}_a$ which continuously alters the system energy balance since \mathbf{H}_a is varying in time (Bertotti 1998). The stability of a given domain configuration is sooner or later destroyed by the applied field variation. The domain structure becomes unstable and it spontaneously evolves toward some new configuration. This rearrangement may be quite localized in space, with a small domain wall segment jumping to a neighboring stable position, or may involve the whole domain structure. As a sequence of spontaneous rearrangement of the domain structure, a random chain of voltage spikes—Barkhausen jumps—appears across the winding. The stochastic nature of the Barkhausen jumps leads to variations of amplitude, shape, duration, and phase for the different excitation cycles. As a result, fluctuations of the hysteresis loop are observed at the cyclic magnetization reversals.

Plenty of experimental and theoretical studies of fluxgates and magnetic amplifiers allow us to find correlations between the noise level and the basic parameters of soft magnetic materials. An excellent review of these dependencies is given in Musmann and Afanassiev (2010) and, as a result, a set of requirements was formed; these are (a) close to zero magnetostriction and anisotropy constants, (b) low values of the saturation induction, coercive force and power losses at re-magnetization, (c) maximal initial permeability, and (d) the Curie temperature as low as possible. Besides, the magnetic core has to be free from mechanical defects and stresses; further, each part of the core has to be magnetized uniformly. The proper selection of the magnetic core, which satisfies these requirements, as a rule means that variations of the free energy landscape in the magnetic material are as small as possible. Consequently there is a low level of Barkhausen jumps, and good reproducibility of the hysteresis loop from cycle to cycle may be observed.

We believe that the free energy landscape in the magnetic material may be compared with the domains' surface roughness, and the energy of thermal fluctuations may be attributed to "grease," which smoothes the roughness and decreases the friction between domain walls. This may explain the thermal dependence of the Barkhausen jumps and the fact that the lower Curie temperature is, the lower is the magnetic noise. It also shows the way to reduce the magnetic noise; this is to manufacture the magnetic material with a structure which will create the right conditions for the magnetic domain walls to decrease the friction between them as much as possible. Then they glide easily and uniformly when changing domains orientation at magnetic field reversals.

Ideally, such a material may be represented as a "solid liquid" with freely floating uniform magnetic domains without friction between the walls. It is obvious that it is not possible to create such a material, but the best materials have to approach this model as much as possible. It is also clear that the omnipresent structural irregularities in permalloys or vacancies in amorphous alloys will increase this friction.

To reduce the specific NL of the materials, several post-melting processing technologies were developed. A set of experiments conducted by many investigators has shown that the best results are obtained by annealing the magnetic materials in a vacuum or in an inert gas (argon, for example), and by applying for the entire annealing time the alternative magnetic field, imitating the core excitation field during FGM operation. It was found that each alloy has a specific annealing temperature peak, which is sometimes rather narrow, at which the NL becomes minimal (Fig. 3). If we accept the proposed “solid liquid” model, this mechanism for decreasing the NL has a clear physical explanation: permanent re-magnetization of the domains leads to the domain walls “smoothing” after numerous mutual frictions. There are favorable structural improvements for the homogenization of transitions, and the rise of temperature gives the necessary energy for liquidation of the material structural impurities. This specific temperature for each alloy, after which the noise level starts to increase again, is probably caused by the beginning of partial crystallization of the amorphous phase (Yang et al. 1997). As a result, local changes of the magnetic domain structure are formed after cooling, which increases the NL.

This postulate found unexpected confirmation in the results of space missions. Acuna (2002) was the first to report that during FGM operation in space its NL decreases with time; he attributed this to the relaxation of mechanical stresses in the core material in the space environment. Not rejecting this assumption, we would like to highlight another possible mechanism for the noise improvement. We studied in detail some conditions in which the core material is in space—vacuum and radiation. The long-term tests of a FGM sensor in a vacuum chamber (both in operation and in switched off conditions) showed no influence of this parameter on the NL. The influence of radiation, the dose of which was selected to be approximately equal to the yearly dose in near-Earth orbit (~ 10 krad), revealed interesting facts: the magnetic material itself and the FGM sensor in the non-operational state had not shown any dependence on radiation, whereas this dose applied to the operating FGM sensor led to the marked reduction of the NL. This new effect, named “gamma-magnetic normalization” (term proposed by Dr R. Berkman), can also be explained by the suggested model: the mechanism is the same as above, but because γ -quanta have much greater energy than thermal quanta, more “rigid” impurities are eliminated by γ -radiation action. Because the number of impurities in the material normally

Fig. 3 Noise dependence (at 1 Hz) vs annealing temperature for Co-based amorphous alloys

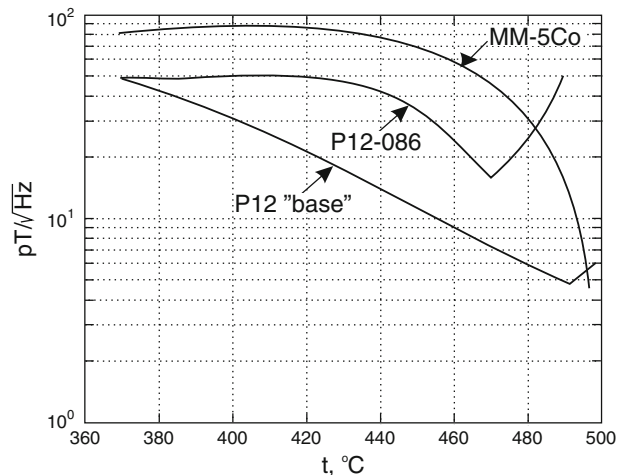
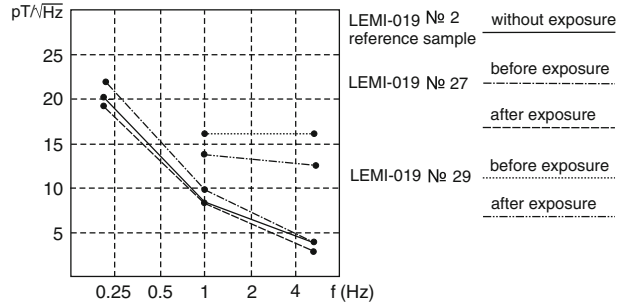


Fig. 4 The noise level changes after γ -radiation action



decreases with their “rigidity,” the NL improvement by gamma-magnetic normalization is expected to be not very big. This was confirmed in our experiments in the laboratory (Fig. 4): the NL decreased by $\sim 15\text{--}20\%$ only after the 10 krad dose of radiation was applied. It is possible to assume that, with time, because more and more energetic γ -quanta may occur, the NL has a further tendency to decrease slightly. Unfortunately, no numerical data about noise level reduction in space magnetometers has been found.

2.1.2 Some Methods of Magnetic Noise Suppression

Koch et al. (1999) estimated the theoretically lowest possible white noise of second-harmonic fluxgates with a single-domain magnetic core. This assumes the absence of the Barkhausen jumps and the NL calculation based only on the equilibrium thermal fluctuations. In this case, the noise is mainly caused by the thermal energy of the spin system and the conduction electrons (Bittel 1969). Using the Landau-Lifshitz-Gilbert equation Koch et al. (1999) had simulated magnetization fluctuations and found them to be inversely proportional to the core volume and to increase approximately linearly with the intrinsic losses in the core. It was also found that the white noise of a single-domain FGS with a volume 20 mm^3 could be as small as $0.1\text{ pT/Hz}^{0.5}$, if the thermal noise of the eddy currents is limited by the appropriate selection of core geometry and material.

Sets of rod- and ring-core fluxgates were fabricated for achieving the predicted noise level (Koch and Rozen 2001). In order to create the single-domain state, a DC current was passed through the copper winding placed inside the tubular magnetic core in the case of the rod-core sensor and directly through the amorphous magnetic wire, which formed the core of the ring-core sensor. This DC current generated the permanent circumferential bias field in the core, whereas the AC current through the conventional excitation winding was periodically driving the core into saturation along its axis. Significant improvement of the noise level of the biased cores was observed over the unbiased ones. Nevertheless, the values of the noise level achieved at 1 Hz— $1.4\text{ pT/Hz}^{0.5}$ for ring core and $3.5\text{ pT/Hz}^{0.5}$ for rod core—still considerably exceed the thermal equilibrium predictions.

The attempts to suppress Barkhausen fluctuations using special excitation modes and/or magnetic materials were made by other researchers too. For instance, noise $\sim 0.4\text{ pT/Hz}^{0.5}$ with the help of the circularly excited single-domain yttrium garnet film core with the volume 0.25 mm^3 was measured by Vetoshko et al. (2003). They showed that the measured noise level is caused by thermal fluctuations of the sensing coil whereas the thermal noise of the magnetic core has to be $\sim 5\text{ fT/Hz}^{0.5}$!. The operational principle and the electronic unit structure of this instrument differ considerably from those of conventional FGMs; for this reason it is named the “flux-spin” magnetometer.

Another example is the rod-core fluxgate sensor with double excitation based on the Co-based amorphous wires, which demonstrates a noise of $1.6 \text{ pT/Hz}^{0.5}$ at the core volume 0.8 mm^3 (Ioan et al. 2004). The described excitation mode, however, had not provided any advantages when permalloy wires were used instead of amorphous ones. This peculiarity was explained by a specific magnetic domain structure of the amorphous wire used—it consisted of a central axially magnetized mono-domain core region and an outer shell with circumferentially magnetized domains (Ioan et al. 2004). Applying a current through the wires, the shell regions were also kept saturated or in the mono-domain state. Under the combined magnetization by axial and circumferential fields, the magnetization reversal was performed by rotation in both regions of the wire.

The coherent rotation of magnetization was also exploited in the fundamental-mode orthogonal fluxgate for noise level decreasing (Sasada and Kashima 2009; Paperno 2004; Paperno et al. 2008). Using amorphous wire with uniaxial anisotropy, the noise level $10 \text{ pT/Hz}^{0.5}$ at the core volume 0.23 mm^3 was achieved (Paperno 2004). In order to avoid magnetization reversal, the core was excited by the unipolar field along a minor hysteresis loop near one of the saturated states. As a result, the fundamental-mode orthogonal fluxgate has a considerable offset; to cancel this, one of several methods was used (Weiss and Paperno 2011). Another probable drawback of the fundamental-mode sensor with respect to the second-harmonic fluxgate is a weaker immunity to the false detection of the feed-through signal, because the useful and parasitic signals share the same frequency bands.

These methods of avoiding domain wall displacement at magnetization use the special excitation modes to keep the material as close as possible to the single-domain state. To the best of our knowledge, such magnetometers exist only as experimental examples and are not commercially available. Many important parameters of these magnetometers, such as their long-term thermal stability and power consumption, remain unknown.

The idea to suppress the domain wall movements and to manage magnetization reversal solely by the coherent rotation was the basis for using in parallel fluxgates a magnetic core with a hard axis of magnetization along the excitation field direction (Nielsen et al. 1991; Moldovanu et al. 2000; Tejedor et al. 1995). The uniaxial anisotropy produced by suitable stress annealing causes a specific domain structure in amorphous ribbons—the stripe-like domains extended along the ribbon width from one edge to the other. As a magnetizing field is applied along the ribbon axis, the domain pattern does not change until it disappears at saturation. Thus, the domain walls are fixed in the stable position, and the magnetization reversal is performed mainly by the rotation process. The achieved noise level was approximately from 6 to $10 \text{ pT/Hz}^{0.5}$ both for the ring-core FGS with the magnetic core volume 16 mm^3 (Nielsen et al. 1991) and for the rod-core sensor with the magnetic material volume 4 mm^3 (Moldovanu et al. 2000).

2.1.3 Noise Level Comparison of the Magnetic Materials

As we can see, there are two strategies for making low-noise FGSs. The first is to create a high-quality multi-domain magnetic material with the uniform distribution of the free energy landscape and, as a result, with freely moving domain walls. The other approach is to avoid domain wall movements at all by keeping the material in the single-domain state applying special excitation modes or by fixing domain walls in materials with a uniaxial anisotropy. It has to be noted that the benefits from the suppression of domain walls movements and an associated Barkhausen noise decrease could be obtained if the magnetization rotations are highly repeatable from cycle to cycle and other processes such as domain annihilation and nucleation are absent or reproducible too. From this point of view,

for both approaches the magnetic material with the lowest level of structural imperfections is required. The important difference between the two approaches is the requirement for anisotropy of the magnetic material. In the first case, an isotropic ferromagnetic has to be used as the core material, whereas some kind of magnetic material anisotropy has to be present according to the strategy of suppressing domain walls movements.

It is interesting that the aforementioned noise-minimizing approaches should lead to the opposite dependencies of the FGS NL on temperature. The conventional FGS noise level drops as the sensor temperature is getting close to the Curie point of the core magnetic material (Berkman and Afanasenko 1976; Shirae 1984). At the total Barkhausen noise suppression, the FGS noise level will be caused only by thermal fluctuations, so the noise power should be proportional to the sensor temperature.

We may therefore state that, for both strategies, the FGM NL mainly depends on the quality of the magnetic material used for the FGS core and its excitation mode. In order to compare the magnetic materials, let us use the specific noise level parameter C_B as a criterion of their excellence. The parameter C_B refers to the noise spectral density b_0 and to the magnetic core volume V_F as follows: $C_B = \sqrt{b_0 V_F}$.

Let us note that there are different opinions about FGM NL dependence on the sensor core volume V_F . For thermally generated noise, the dependence $b_0 \equiv V_F^{-1}$ is theoretically substantiated (Koch et al. 1999; Vetoshko et al. 2003).

The theoretical and experimental studies of the magnetic amplifier noise (Musmann and Afanasiev 2010) and fluxgates (Berkman 1999) also showed that the dependence $b_0 \equiv V_F^{-1}$ is generally valid for the noises of Barkhausen origin. But it is necessary to underline that this dependence is observed only when the FGS core maintains a similar topology when changing its volume, that is, the core dimensions ratio remains approximately the same as the volume increment. This is confirmed in the experiment made by O. Rasmussen (private communication): changing the core tapes number from 2 to 4, he obtained a NL decrease corresponding to the expression given above, but a further increase in tapes number from 4 to 8 did not reveal this dependence—we believe that this is because the core topology was already strongly violated. This may explain why the NL of the sensors using a short and thick core is greater than for sensors with elongated cores or thin ring cores with the same V_F .

In the Table 1, the C_B parameter values for the best known magnetic materials are given. In the upper part of Table 1, the materials are selected in accordance with the classical criteria of minimal variations of the free energy landscape. Next shown are the ferromagnetics with uniaxial anisotropy, which creates a hard magnetization axis along the excitation field. Then there is a group of materials with particular magnetic anisotropy and complicated excitation modes. Theoretical expectations of the magnetization thermal noise complete Table 1.

It follows from Table 1 that the materials with uniaxial anisotropy used in fluxgates with parallel excitation (Nielsen et al. 1991, Moldovanu et al. 2000) have no advantages over the isotropic soft materials selected in accordance with the classical approach. It is also seen that the group of materials subjected to the special excitation modes in general has a lower value of the parameter C_B than the classically selected materials with conventional excitation mode. This result should stimulate further investigations and the development of sensors with completely suppressed Barkhausen noise. As we can see, the present-day implementations of this strategy are far from the theoretically predicted limits. Thus, achieving the full capabilities of this approach will allow FGSs to be created with really outstanding noise characteristics.

Table 1 Comparison of magnetic materials by their specific noise levels

Magnetic material	$C_B \times 10^{15},$ $T \cdot m^{3/2} \cdot Hz^{-1/2}$
Permalloy (Ni ₈₃ V ₅ Fe ₁₁) (Berkman 1999)	0.4–0.8
Mo-Permalloy (Ni ₈₁ Mo ₆ Fe) (Magson 2008)	0.23
Co ₆₈ Fe ₃ Cr ₃ Si _{1.5} B ₁₂ (annealed in the longitudinal AC magnetic field, LC ISR)	0.2–0.36
Ni ₇₂ Mo ₃ Cu ₁₄ Cr ₂ Fe ₉ near Curie point (magnetic modulator, Berkman and Afanassenko 1976)	0.12
Co _{62.3} Fe _{2.8} Cr ₇ Si _{13.9} B _{13.9} near Curie point (Shirae 1984)	0.11
Co _{66.5} Fe _{3.5} Si ₁₂ B ₁₈ (stress annealed) (Nielsen et al. 1991)	0.7–1.3
Vitrovac6025 (stress annealed) (Moldovanu et al. 2000)	0.4
Co _{68.18} Fe _{4.32} Si _{12.5} B ₁₅ (double excitation, Ioan et al. 2004)	0.045
AC-20 from UNITICA Ltd (fundamental-mode orthogonal fluxgate, Paperno 2004)	0.15
Amorphous wire in the ring-core FGS with DC bias field (Koch and Rozen 2001)	0.14
Yttrium garnet film, circular excitation (Vetoshko et al. 2003)	0.006
Theoretical limit for DC field biased parallel FGS (Koch et al. 1999)	0.014
Theoretical limit for circularly excited yttrium garnet film core (Vetoshko et al. 2003)	0.00008

According to our opinion, further NL improvement of FGSs with traditional excitation mode is possible by applying smart signal processing procedures in the time domain instead of the usually used second-harmonic useful signal detection. The time domain detection procedure will allow the distribution of the Barkhausen noise to be taken into account along the excitation cycle; the precise extraction of the useful signal solely at the parts of this cycle where the Barkhausen noise has the lowest amplitude should be possible.

2.2 Excitation Mode Selection

As was mentioned above, in the conventional saturation mode the FGS magnetic core has to be deeply saturated twice per period for minimizing sensor drifts and noises. Besides, the shape of the excitation voltage has to be relatively independent of the variations of the magnetic core parameters; otherwise, both the voltage spectrum across the secondary coil and the sensor sensitivity will vary (Berkman 1999). That is why great attention was paid by many investigators to develop the best possible excitation mode. The peculiarities of different types of the excitation modes were thoroughly studied at the early stages of FGM development (Musmann and Afanassiev 2010) and, as a result, as Table 2 shows, a so-called “ferroresonance excitation mode” (FEM) was proposed as the optimal one (Berkman et al. 1972; Korepanov et al. 1997).

The simplest circuit realizing the FEM and the plots of currents and voltages in this mode are given in Fig. 5a and b. The peculiarity of the FEM was the use of the nonlinearity of the ferromagnetic resonance circuit when the impedance of the coil L_e with high permeability ferromagnetic core differs by many times during the periods of the saturated and non-saturated states of this core. By this, the driving current i_g may have a sinusoidal shape, which makes it much easier to damp the second harmonic of the excitation current frequency, and the resulting excitation voltage u_e has the shape very close to the rectangular one, which was generally accepted as the best possible (Musmann and Afanassiev 2010) to reduce the FGM noise. As may be seen in Fig. 5, the resulting excitation current amplitude i_e greatly surpasses the driving current amplitude i_g , which is very favorable

Table 2 Comparison of the FGS excitation modes

Parameter	Excitation mode						
	Current (shape)				Voltage (shape)		
	Sinusoidal	Triangular	Trapezoidal	Stepwise rectangular	Sinusoidal	Triangular	FEM
Sensitivity threshold	+	0	0	0	++	+	++
Even harmonic error	+	0	0	0	++	+	++
Generator voltage changes error	+	+	+	++	0	0	++
Perming error	0	0	0	+	+	+	++
Sensitivity stability	0	0	0	++	+	+	++
Rapidity	+	+	0	0	++	++	++
Self-heating of FGS	0	0	0	0	+	+	++
Realization simplicity	++	+	0	0	++	++	+
Analysis and calculation simplicity	++	++	++	++	0	+	0

0—unsatisfactory value of the parameter; +—satisfactory value of the parameter; ++—good value of the parameter

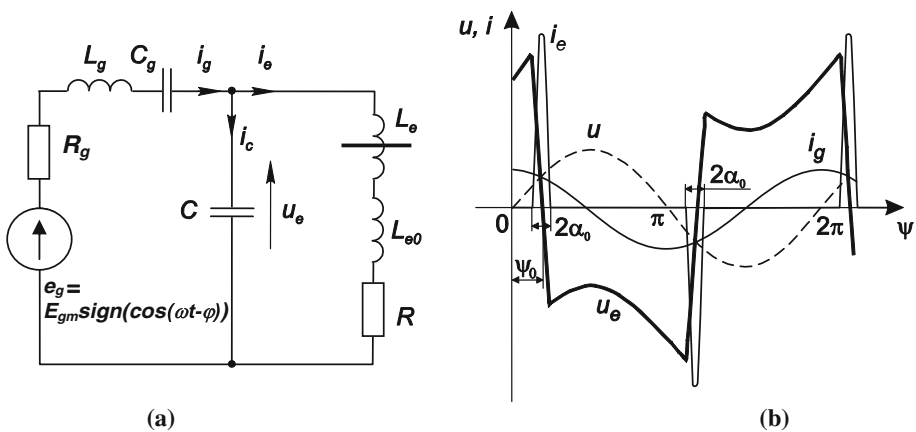


Fig. 5 The circuit for realizing the FEM (a) and the plots of the currents and voltages during the FEM (b). L_{e0} and L_e —inductance of the excitation winding at the saturated and unsaturated states of the magnetic core, R —equivalent resistance of the losses in the core and the excitation winding, C —tank capacitor, C_g and L_g —the elements of the tuned series circuit at the oscillation frequency (as a rule $C_g < C$), R_g —equivalent resistance of the excitation generator, including losses in C_g and L_g

both for deep saturation of the FGM core and for power economy: in a high-class FGM, at peak current in the pulse up to 1 A, the mean consumed current by the excitation circuit in this mode is only about 5 mA! For a lower class FGM, this gain may be still higher. The

ability to provide the strong excitation field makes the FEM suitable for sensors which should withstand an overload by a large magnetic field: the perming error—the zero offset after overload—is very small for sensors operated in the FEM.

2.3 Thermal Drift

The thermal drift is also an important FGM parameter. In a properly designed device, it is mainly determined by following sources:

- (1) thermal stability of the electronic components,
- (2) mechanical stability of the FGS housing, and
- (3) uniformity of the compensation field.

The advanced modern electronic circuit development practically excludes the input of the electronic unit in the total thermal drift of FGM. In modern FGMs, it is mainly determined by the thermal influence on the FGS core position and compensation field homogeneity: even tiny movements of the sensor core in the magnetic field of the Earth or in the compensation winding field may cause a big error. For example, the deviation of the sensor axis by only 10 arcsecond may lead to a ~ 2.5 nT offset in the transverse field. This error source—sensor movement—may be minimized by constructing the FGS housing using materials whose thermal expansion coefficient is as small as possible, namely marble and/or quartz glass. The most widespread observatory magnetometers DFM from Denmark are using just this combination (DTU 2009). Modern technology offers still better materials of the glass–ceramic class, the thermal coefficient of which is equal to zero and the machining of which, though complicated, allows the FGS housing and its components to be made from this material (Fig. 6), so that this kind of error is greatly reduced.

Another way to decrease the sensor core tilt effect is the so-called “volume or vector compensation,” when the compensation windings are placed on the sphere or cube within which the component sensors are fixed (Primdahl and Jensen 1982). The compensation coils are specially designed to create a highly uniform magnetic field, which almost completely cancels the measured field in the whole volume of the flux-gate elements. This construction is used in advanced space magnetometers (Fig. 7); it is rather expensive and difficult to realize.



Fig. 6 Three-component FGS with glass–ceramic housing

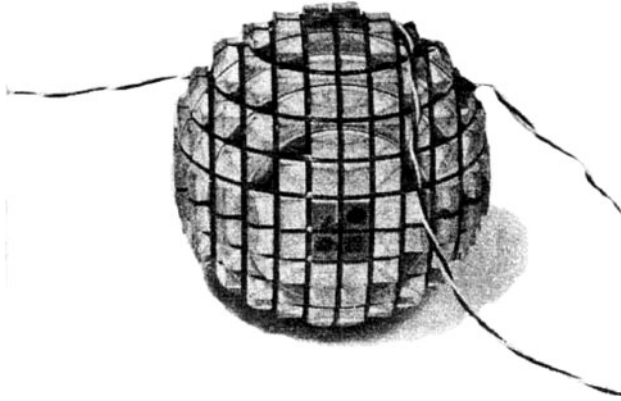


Fig. 7 Compact spherical coil (Primdahl and Jensen 1982)

The next most important error source is the core shift and change of its effective length inside the compensation winding. The latter factor could be, for example, caused by deviation of the excitation field with temperature and, as a result, a different level of core edges' saturation. As soon as the compensation field of the coil, the length of which is the same as that of the core, cannot be uniform in principle, deviations of the core length and/or position inside the coil under the influence of temperature changes will cause important signals.

In contrast to making the highly uniform field using complicated construction of the compensation windings (Primdahl and Jensen 1982), other much simpler ways may be proposed, at least for the bar-core and racetrack sensors. One such way consists in creating the compensation field of such a shape that, in the regions of the core ends, the created magnetic field will have close to zero spatial derivatives and hence will minimize the influence of sensor core shift and length variations. To fulfill this, the optimal type of non-uniformity of the compensation field $H(z)$ has to meet the conditions (Marusenkov 2006):

$$\frac{1}{l_e} \int_0^{l_e} H(z) dz = H(l_e), \quad (2)$$

$$\left. \frac{dH(z)}{dz} \right|_{l_e} = 0, \quad (3)$$

where l_e is the half of the effective length of FGS core. An example of such a compensation field shape is given in Fig. 8.

If the conditions (2, 3) are fulfilled, the small deviations of the length or/and position of the FGS core have practically no influence on the value of the applied compensation field averaged along the core length. The tests performed with different shapes of non-uniformity of the compensation field (Fig. 9a) confirmed the efficiency of the proposed approach.

As a varying factor, the amplitude of the fluxgate excitation field was used, because it is easy to control and partially represents the change of the sensor excitation behavior due to the temperature. As is clearly seen (Fig. 9b), at the optimal shape of the non-uniformity

Fig. 8 Distribution of the compensation field along the FGS sensor axis

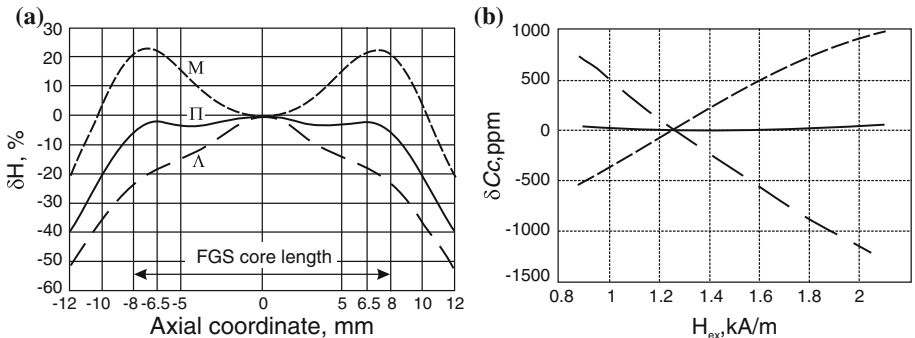
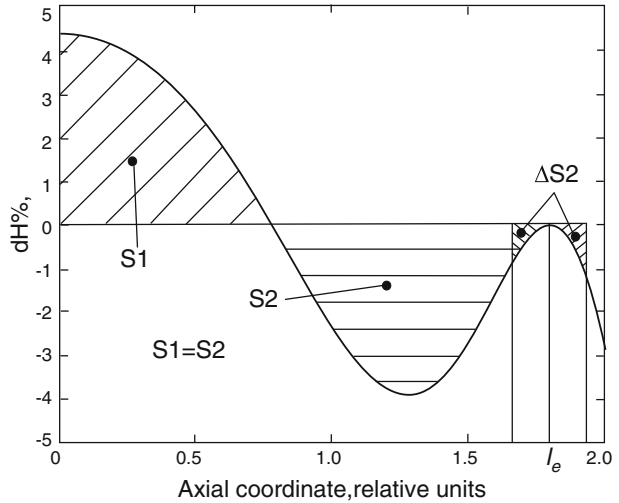


Fig. 9 Types of compensation field non-uniformity (a) and corresponding relative changes of compensation coil constant C_c (b)

(marked “ π ” in Fig. 9a) the equivalent compensation coil constant C_c is practically independent of excitation field variations.

The efficiency of such an optimized design of the compensation coil was confirmed in miniature three-component FGS with vector compensation of the measured field. This sensor was specially developed for the small magnetometer in low-mass experiment (SMILE)—the novel instrument created in the collaboration with the Royal Institute of Technology, Sweden (Forslund et al. 2008). In spite of its very low weight (<20 g) and small dimensions (20 × 20 × 20 mm), the thermal drift for this sensor was experimentally measured as <0.1 nT/ °C.

2.4 Power Consumption

FGMs are far ahead of magnetometers of other types, if one seeks for the best balance between the noise level (at DC and low frequencies) and the power consumption. The development and rapid improvement of modern electronic components allows very low-power electronic units to be built for FGMs (Delevoeye et al. 2008; Forslund et al. 2008; Magnes et al. 2008). The limiting factor for the further reduction of power is the power consumed by the fluxgate sensor itself. Here, two major power “users” may be determined as follows:

- (1) power losses in the core, and
- (2) power losses in the winding.

The analysis of these showed the following situation. The power losses per cycle in the magnetic core of unit volume during magnetization reversal consist of three components (Bertotti 1998):

$$\frac{P}{f} = C_0 + C_1 f + C_2 \sqrt{f} \quad (4)$$

where $C_0 \propto M_{\max}^2$ —the coefficient of the hysteresis loss; $C_1 \propto M_{\max}^2$ —the coefficient of the classical loss due to the eddy currents in the perfectly homogenous material; $C_2 \propto M_{\max}^{1/2}$ —the coefficient of the excess loss connected to the eddy currents surrounding the active magnetic domain walls in motion under the action of the external field; M_{\max} peak magnetization, $\mu_0 M_{\max} = B_s$ at fluxgate excitation; B_s —saturation induction.

In the frequency band 1–20 kHz commonly used for fluxgate excitation at moderate peak magnetization M_{\max} , the experimenters report that excess loss generally exceeds the hysteresis and classical losses (Magni et al. 2011; Appino et al. 2004; Flohrer et al. 2006). As the excess loss dependence on the peak magnetization is weaker than that of the hysteresis and eddy currents losses, its relative contribution to the total losses decreases while the magnetization reversal is performed along the major hysteresis loop and $\mu_0 M_{\max} = B_s$. The excess loss depends on the particular domain structure of the core (Bertotti 1988); even the same magnetic material may demonstrate different behavior of the excess losses after different preparation procedures (annealing conditions, stress, surface polishing, etc.) (Flohrer et al. 2006; Ferrara et al. 1997). Therefore, it is rather difficult to give a general expression for excess losses regardless of the peculiarities of the particular specimen.

Our experimental study allowed us to reveal that for flux-gate magnetic cores produced from polycrystalline permalloy $\text{Ni}_{83}\text{V}_5\text{Fe}_{11}$ and Co-based alloy, the observed power losses are in good agreement with calculations based only on the hysteresis and classical loss contributions (Marusenkov 2003). We therefore neglect excess losses and calculate the total power consumption as a sum of hysteresis and classical parts, keeping in mind, however, that the obtained result could be a slight underestimate. It is a common recommendation that the magnetic materials used in fluxgates have to keep low static coercivity H_c (Musmann and Afanassiev 2010), which simultaneously means low hysteresis losses. For example, the hysteresis losses in polycrystalline alloys with high nickel content do not exceed 20 J/m^3 (using data from Musmann and Afanassiev 2010) and could be even less in amorphous and nanocrystalline alloys (Appino et al. 2004; Flohrer et al. 2006).

Let us estimate the classical losses for a magnetic material with a step-like magnetization law. In this case, the applied excitation field changes during magnetization from $-B_s$ to $+B_s$ according to the law (Bertotti 1998):

$$H_a(t) = \frac{\sigma \Delta^2}{8} \left| \frac{dB}{dt} \right| \left(\frac{B(t)}{B_s} + 1 \right), \tag{5}$$

where σ —specific conductivity of magnetic material; Δ —thickness of the magnetic ribbon; $\left| \frac{dB}{dt} \right|$ —absolute value of the magnetic induction rate during transition between saturated states.

In the FEM, the voltage across the excitation winding has an approximately rectangular shape (Fig. 5b). This means that the magnetic induction rate is constant during magnetization reversal and is equal to

$$\left| \frac{dB}{dt} \right| = 4f_{ex}B_s \left(\frac{\pi}{\pi - 2\alpha_0} \right), \tag{6}$$

where $2\alpha_0$ —relative width of the excitation pulse (Fig. 5b); f_{ex} —excitation frequency. In this case, the dynamical hysteresis loop looks like a parallelogram and the classical losses are given by the expression (Marusenkov 2003):

$$P^{cl} = \frac{2\pi\sigma\Delta^2 f_{ex}^2 B_s^2 V_F}{\pi - 2\alpha_0}, \tag{7}$$

where V_F —volume of the core.

Expressing core volume V through its length l and the permeability of the core shape as μ_s , the total power losses in the fluxgate core may be calculated as follows:

$$P_c = \left(4B_s H_c f_{ex} + \frac{2\pi\sigma\Delta^2 f_{ex}^2 B_s^2}{\pi - 2\alpha_0} \right) \frac{l^3}{5\mu_s}, \tag{8}$$

where $\mu_s = l^2/(5S_c)$ —relative permeability of the core shape for bar-core and racetrack FGS; S_c —cross-section of the core.

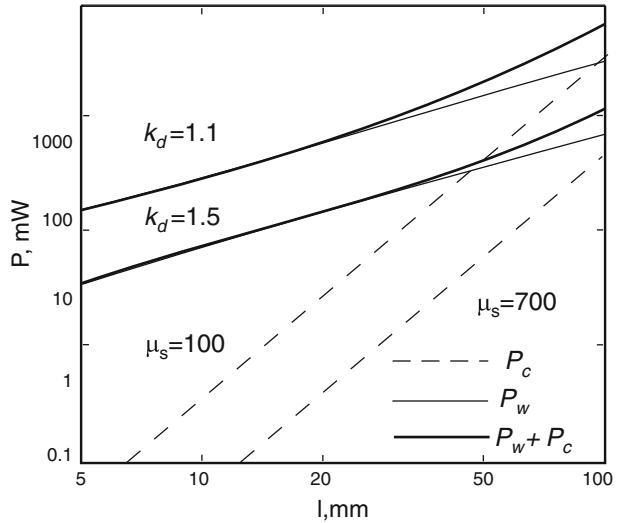
The power dissipation P_w in the FGS winding as a function of the magnetizing force amplitude H_m can be estimated using the expression (Marusenkov 2003):

$$P_w = \frac{2\pi(k_d + 1)}{k_A^2 k_H^2 k_w (k_d - 1)} \rho H_m^2 l = KH_m^2 l, \tag{9}$$

where $k_A = I_m/I_{rms} \cong \sqrt{\frac{\pi}{\alpha_0}}$ —peak factor of the excitation current, k_w —filling factor of the excitation winding, k_d —ratio between outer and inner diameters of the excitation winding, k_H —factor of excitation field decrease due to its non-uniformity along the core ($k_H = 0.7-0.9$ for bar-core sensors and $k_H \rightarrow 1$ for ring-core and racetrack sensors), and ρ —specific resistivity of copper.

For the given sensor length l and the magnetizing force amplitude H_m , only the factors k_A , k_H , k_w , and k_d may be changed—according to the expression (9), they have to be increased to minimize P_w . However, the factors k_H and k_w physically cannot exceed 1 and approaching this value is limited by technological problems. Increasing the factor k_A —the peak factor of the excitation current—is possible only by decreasing the relative width of the excitation pulse, which, in turn, could negatively influence the sensitivity and the noise level of the sensor. Therefore, the only term which may be controlled independently (within some limits) on NL is k_d : we may increase it using thicker wire or, in other words, increasing the weight of copper. It appears that P_w falls very rapidly when the factor k_d changes from the initial value (close to 1) to the value ~ 2 . Further increasing the winding thickness is usually prevented by technological problems. The efficiency of such an

Fig. 10 Power consumption for FGS excitation. Core material— $\text{Ni}_{83}\text{V}_5\text{Fe}_{11}$; $B_s = 0.52$ T; $H_{eq} = 8.7$ A/m; $f = 10$ kHz; $\Delta = 0.02$ mm; $H_m = 1,500$ A/m; $k_w = 0.5$; $K_A = 2$; $k_H = 0.9$



approach is demonstrated in Fig. 10, where the dependences of the total excitation power and its components on sensor core length are presented. The total power is plotted by thick lines for two cases: $k_d = 1.1$ and $\mu_s = 100$ (the upper thick line) and $k_d = 1.5$ and $\mu_s = 1,000$ (the lower thick line). The dotted and thin lines are the contributions of P_c and P_w , respectively. As we can see, by increasing the factor k_d from 1.1 to 1.5 it is possible to save almost 80 % of the power losses in the winding.

For a typical construction of FGS ($k_d = 1.1$ and $\mu_s = 100, \dots, 1,000$), Fig. 10 shows that over a wide range of sensor lengths the majority of the excitation power dissipates in the winding. So, to increase the coefficient k_d or, in other words, the volume of copper in the winding is also a good way to decrease the total power consumption considerably. This may be realized most easily for a bar-core FGS.

3 Applications in Geophysics

As was noted above, flux-gate magnetometers are the most widespread devices today for vector measurements of a DC magnetic field and its slow fluctuations. Other quickly developing types, for example, Hall effect or giant magnetoresistive (GMR) and magnetoimpedance (GMI) magnetometers, have several advantages. However, using a set of parameters such as noise level, power consumption, and price, it is found that they are still not competitive.

One of the most impressive examples may be low-power FGMs. The development of modern technology and applications more and more often requires magnetometers with as low as possible a power consumption but with a sufficiently low NL. A possible way to decrease power consumption was shown in the preceding section. Using this approach, a set of low-power FGMs was manufactured with the power consumption ranging from only 1.5–22 mW per component. We have collected in Table 3 the best known FGMs that retain their outstanding position among modern analog flux-gate magnetometers and having the best combination of parameters such as noise and power consumption. Using

Table 3 Power/noise data of best low-power FGMs

Manufacturer	Type	Number of components	Power, mW (at 50,000 nT)		Noise, pT/Hz ^{1/2} (at 1 Hz)
			Total	Referred to one component	
Bartington Instruments (Bartington 2011)	MAG566	3	27	9	200
	MAG-01 MS	1	328	328	6
	MAG648	3	15	5	10
	MAG-03	3	480	160	6
Stefan Mayer Instruments (Mayer 2011)	FL3-100	3	592	197	10
	FLC3-70	3	30	10	120
Billingsley Aerospace and Defense (Billingsley 2008)	TFM100-G2	3	375	208 (125)	12
	TFM65-VQS	3	504	168	20
Lviv Centre of Institute for Space Research (LC ISR 2009)	LEMI-019	1	30	30	7
	LEMI-011	3	25	8.3	150
	LEMI-031	3	10	3.3	25 (8 for low-noise version)
CEA-LETI (Delevoye et al. 2008)	CEA-LETI	3	3	3	5,000
Narod (private communication 2011)	PC-104	3	240	80	6

these data, their excellence level is illustrated in Fig. 11, where the so-called “excellence line” (dashed) is constructed as a mean value of all presented noise/power parameters and every point corresponds to a given magnetometer position relative to this line. The points above the line classify the corresponding FGM as worse than average, and the points below it as better than average; the further that the point is from the line, the higher is that FGM’s excellence.

The methods described to raise the FGM main parameters level were also used for the construction of probably the less consuming among known automated geophysical magnetovariational station LEMI-018 (LCISR 2009), see Fig. 11. The combination of very low noise level (<10 pT at 1 Hz) and power consumption (<0.6 W), together with GPS-synchronization and sufficient internal memory for more than 1 year of independent operation, makes it very convenient for long-term autonomous registration of variations of the Earth’s magnetic field, especially in remote areas.

Another successful example of the development of a high-class FGM is the unique observatory variometer LEMI-025 supporting a true 1-s INTERMAGNET standard (Korepanov et al. 2008). Together with its super-low noise level (typically below ~3 pT), this allows the registration of 1-s data at every integral second to within an error of less than ±5 ms and mains interference damping of more than 120 dB. All this makes it especially efficient for coordinated measurements using satellite-borne magnetometers in the present and future scientific missions (SWARM, for example).

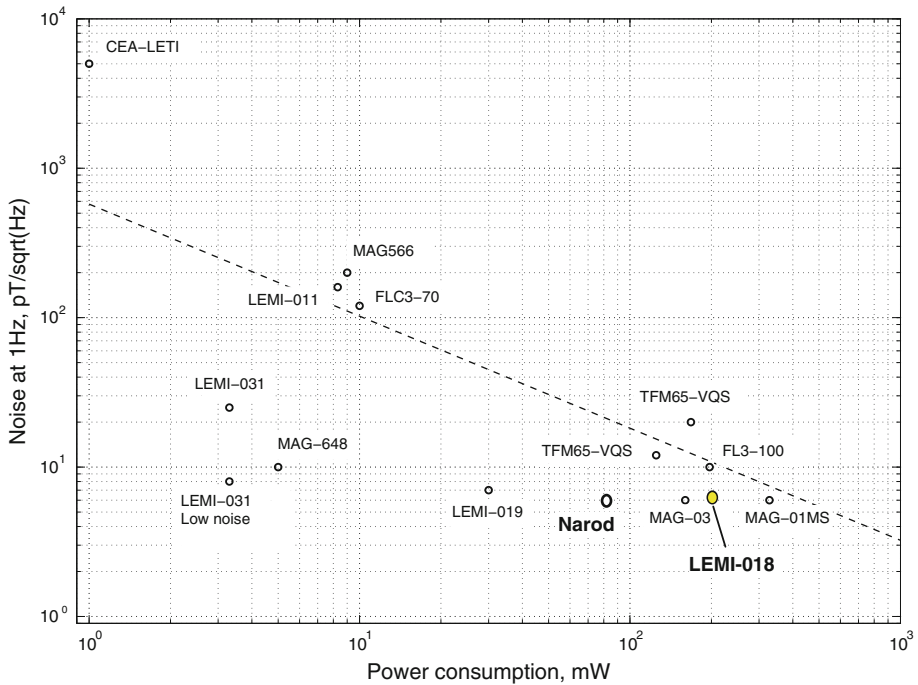


Fig. 11 Comparison of the modern FGMs by noise level versus power consumption criteria

4 Conclusions

To create an FGM with the lowest possible NL, attention has to be paid primarily to the selection of the best material for the FGS core, its annealing mode and its excitation mode. Also, the proper selection of FGS housing material has to be made. It is assumed that the quality of electronic components applied during FGM manufacture is appropriate so that their effect on the final performance is insignificant.

The further improvement of FGM noise parameters is expected using special excitation modes, which allow Barkhausen noise in the magnetic core to be avoided. The authors also believe, as stated above, that noise reduction in the conventional FGS with the traditional excitation mode can be achieved by exploiting output signal processing techniques not in the frequency domain, as is usually done, but in the time domain. That allows the Barkhausen noise intensity distribution during the magnetization reversal cycle to be taken into account and also allows the use of an optimal procedure for signal detection. Several investigators are already working on this problem (Delevoeye et al. 2008; Kubik et al. 2007). First results give optimism that, in a few years, commercially available FGMs using this operation mode, with NLs below 1pT , will be produced.

Acknowledgments The authors sincerely thank Dr Hakan Svedhem, ESTEC, for assistance in the experimental verification of the gamma-magnetic normalization effect and to the referees and the editor who helped to improve the quality of the paper very much. This work was partially supported by STCU Grant 5567.

References

- Acuna MM (2002) Space based magnetometers. *Rev Sci Instr* 73(11):3717–3736
- Amalou F, Gijss MAM (2001) Giant magnetoimpedance of chemically thinned and polished magnetic amorphous ribbons. *J Appl Phys* 90:3466–3470
- Appino C, Beatrice C, Ferrara E, Fiorillo F (2004) Magnetization process and magnetic losses in field-annealed amorphous and nanocrystalline ribbons. *J Optoelectron Adv Mater* 6(2):511–521
- Aschenbrenner H, Goubau G (1936) Eine Anordnung zur Registrierung rascher magnetischer Störungen. *Hochfrequenztechnik und Elektroakustik XLV11(6):177–181*
- Auster HU, Lichopoj A, Rustenbach J, Bitterlich H, Fornacon KH, Hillenmaier O, Krause R, Schenk HJ, Auster V (1995) Concept and first results of a digital fluxgate magnetometer. *Meas Sci Technol* 6:477–481
- Bartington Instruments. <http://www.bartington.com>. Accessed 19 April 2011
- Berkman R (1999) Theoretic and experimental investigation of flux-gate magnetometer noise. In: Proceedings of IMEKO-XV World Congress. Osaka, Japan, pp 149–156
- Berkman RY, Afanasenko MP (1976) The magnetic modulators own noise decreasing at the core operation near Curie temperature. *Inf Extr Process* 48:83–87 (in Russian)
- Berkman RY, Bondaruk BL, Fedotov VM (1972) Ferromagnetic resonance excitation mode of the magnetic modulators and flux-gates. *Geophys Instr* 50:20–28 (in Russian)
- Bertotti G (1988) General properties of power losses in soft ferromagnetic material. *IEEE Trans Magn* 24(1):621–630
- Bertotti G (1998) Hysteresis in magnetism. Academic Press, San Diego, CA
- Bertotti G, Fiorillo F, Sassi MP (1981) Barkhausen noise and domain structure dynamics in Si-Fe at different points of the magnetization curve. *J Magn Magn Mater* 23:136–148
- Billingsley Aerospace & Defense (2008) <http://www.magnetometer.com/specs/TFM100%20G2%20Spec%20Sheet%20February%202008.pdf>. Accessed 15 April 2011
- Bittel H (1969) Noise of ferromagnetic materials. *Trans Magn MAG-5* (3): 359–364
- Bohn F, Gündel A, Landgraf FJG, Severino AM, Sommer RL (2007) Magnetostriction, Barkhausen noise and magnetization processes in E110 grade non-oriented electrical steels. *J Magn Magn Mater* 317: 20–28
- Delevoeye E, Audoin M, Beranger M, Cuchet R, Hida R, Jager T (2008) Microfluxgate sensors for high frequency and low power applications. *Sens Actuators A* 145–146:271–277
- DTU Space (2009) http://www.space.dtu.dk/English/Research/Instruments_Systems_Methods/3-axis_Flux_gate_Magnetometer_Model_FGM-FGE.aspx. Accessed 15 April 2011
- Ferrara E, Infortuna A, Magni A, Pasquale M (1997) Structural and magnetic analysis of amorphous Fe₆₄Co₂₁B₁₅ ribbons. *IEEE Trans Magn* 33(5):3781–3783
- Flohrer S, Schafer R, McCord J, Roth S, Schultz L, Fiorillo F, Günther W, Herzer G (2006) Dynamic magnetisation process of nanocrystalline tape wound cores with transverse field-induced anisotropy. *Acta Mater* 54:4693–4698
- Forslund A, Belyayev S, Ivchenko N, Olsson G, Edberg T, Marusenkova A (2008) Miniaturized digital fluxgate magnetometer for small spacecraft applications. *Meas Sci Technol* 19:015202–015211
- Ioan C, Tibu M, Chiriac H (2004) Magnetic noise measurement for Vacquier type fluxgate sensor with double excitation. *J Optoelectron Adv Mater* 6(2):705–708
- Koch RH, Rozen JR (2001) Low-noise flux-gate magnetic-field sensors using ring- and rod-core geometries. *Appl Phys Lett* 73(13):1897–1899
- Koch RH, Deak JG, Grinstein G (1999) Fundamental limits to magnetic field sensitivity of flux-gate magnetic-field sensors. *Appl Phys Lett* 75(24):3862–3864
- Kominis IK, Kornack NW, Allred JC, Romalis MV (2003) A subfemtotesla multichannel atomic magnetometer. *Lett Nat* 422:596–599
- Korepanov V, Berkman R (1999) Comparison of magnetometers efficiency for ELF band. In: Proceedings of the 2nd international conference of measurement, Smolenice, Slovak Republic, pp 195–198
- Korepanov V, Berkman R, Bondaruk B (1997) Advanced flux-gate magnetometer with low drift. XIV IMEKO World Congress. New measurements—challenges and visions, Tampere, Finland, IVA(4) pp 121–126
- Korepanov V, Marusenkova A, Rasson J (2008) A candidate for a new INTERMAGNET standard 1-second variometer: key features and test results. XIII IAGA Geomagnetic Observatory Workshop, Co., USA, p 26

- Kubik J, Janosek M, Ripka P (2007) Low-power fluxgate sensor signal processing using gated differential integrator. *Sens Lett* 5:149–152
- LC ISR (2009) <http://www.isr.lviv.ua/lemi024.htm>. Accessed 5 May 2011
- Liu J, Sellmyer D J, Shindo D (ed) (2006) Nanostructural effects. In: *Handbook of advanced magnetic materials*. Volume 1. Springer
- Magnes W, Oberst M, Valavanoglou A, Hauer H, Hagen C, Jernej I, Neubauer H, Baumjohann W, Pierce D, Means J, Falkner P (2008) Highly integrated front-end electronics for spaceborne fluxgate sensors. *Meas Sci Technol* 19:115801–115813
- Magni A, Fiorino F, Caprile A, Ferrara E, Martino L (2011) Fluxmetrix-magneto-optical approach to broadband energy losses in amorphous ribbons. *J Appl Phys* 109:07A322
- Magson GmbH Ringcores (2008) <http://www.magson.de/pdf/ringcores.pdf>. Accessed 19 April 2008
- Marusenkov AA (2003) The possibilities of increasing efficiency of flux-gate magnetometers. *Ukrainian Metrol J* 1:42–44 (in Russian)
- Marusenkov A (2006) Operation peculiarities of the fluxgate sensor in non-uniform compensation magnetic field. In: *Proceedings of the IXth International Conference “Modern problems of radio engineering, telecommunications and computer science. TCSET’2006*, pp 327–329
- Mayer S Instruments. <http://www.stefan-mayer.com>. Accessed 15 April 2011
- Moldovanu A, Diaconu ED, Moldovanu E, Macovei C, Moldovanu BO, Bayreuther G (2000) The applicability of VITROVAC6025X ribbons for parallel-gated configuration sensors. *Sens Actuators* 81:193–196
- Musmann G, Afanassiev YV (2010) Fluxgate magnetometers for space research. Books on Demand GmbH, Norderstedt: p 292
- Mykolaitis H (1994) Cyclic magnetization noise of nonlinear ferromagnetic cores. *J Magn Magn Mater* 133:520–524
- Narod B (2006) Magnetic permeability and domain structure, and their influence on fluxgate magnetometer noise. In: *Proceedings of EGU General Assembly 2006*, Vienna, Austria
- Nielsen OV, Petersen JR, Fernandez A, Hernando B, Spisak P, Primdahl F, Moser N (1991) Analysis of a fluxgate magnetometer based on metallic glass sensors. *Meas Sci Technol* 2:435–440
- Paperno E (2004) Suppression of magnetic noise in the fundamental-mode orthogonal fluxgate. *Sens Actuators A* 116:405–409
- Paperno E, Weiss E, Plotkin A (2008) A tube-core orthogonal fluxgate operated in fundamental mode. *Trans Magn* 44:4018–4021
- Primdahl F, Jensen AP (1982) Compact spherical coil for flux-gate magnetometer vector feedback. *J Phys E Sci Instrum* 15:221–226
- Ripka P (ed.) (2001) *Magnetic Sensors and Magnetometers*. Artech House
- Sasada I, Kashima H (2009) Simple design for orthogonal fluxgate magnetometer in fundamental mode. *J Magn Soc Jpn* 33(2):43–45
- Shirae K (1984) Noise in amorphous magnetic materials. *IEEE Trans on Magn* 20(5):1299–1301
- Stern DP (2002) A millennium of geomagnetism. *Rev Geophys* 40(3):B1–B30
- Tejedor M, Hernando B, Sánchez ML (1995) Magnetization processes in metallic glasses for fluxgate sensors. *J Magn Magn Mater* 140–144:349–350
- Vetoshko PM, Valeiko VV, Nikitin PI (2003) Epitaxial yttrium iron garnet film as an active medium of an even-harmonic magnetic field transducer. *Sens Actuators A* 106:270–273
- Weiss E, Paperno E (2011) Noise investigation of the orthogonal fluxgate employing alternating direct current bias. *J Appl Phys* 109: 07E529
- Yang JS, Son D, Cho Y, Ryu KS (1997) Soft Magnetic properties of annealed Co-based amorphous $\text{Co}_{66}\text{Fe}_4\text{Ni}_1\text{B}_{15}\text{Si}_{14}$ alloy ribbon. *J Magn* 2(4):130–134